geologica acta

Citation: Saiz, F., Juvany, P., Garcés, M., Beamud, E., López-Blanco, M., 2024. Paleomagnetic study of the curvature of the Segre oblique zone (Southern Pyrenees). Geologica Acta, 22.14, 1-14.
Online ISSN: 1696-5728 DOI: 10.1344/GeologicaActa2024.22.14

Paleomagnetic study of the curvature of the Segre oblique zone (Southern Pyrenees)

Francina Saiz[1,2] **Philémon Juvany**[1,2] **Miguel Garcés**[1,2] **Elisabet Beamud**[2,3]
Miguel López-Blanco[1,2]

[1] **Geomodels Research Institute, Universitat Barcelona, Facultat de Ciències de la Terra**
Martí I Franquès s/n, 08028-Barcelona, Spain

[2] **Departament de Dinàmica de la Terra I de l'Oceà, Universitat Barcelona, Facultat de Ciències de la Terra**
Martí I Franquès s/n, 08028-Barcelona, Spain

[3] **Paleomagnetic Laboratory CCiTUB-ICTJA CSIC**
Barcelona, Spain

ABSTRACT

The origin of the obliquity of the structures at the eastern end of the central South-Pyrenean salient is investigated by means of Paleomagnetism. Earlier paleomagnetic data in the area are poorly distributed and insufficient to describe in detail the amount and age of vertical axis-rotations affecting the region. This work aims to address this issue by focusing on the Palaeocene rocks, whose magnetization if primary would record the entire rotation during the emplacement of the thrust sheet units, improving our understanding of the history of deformation and the paleogeographic implications during the Eocene. In addition to Palaeocene Garumnian facies, late Cretaceous and early Eocene marine facies were also sampled. The characteristic components of the magnetization were obtained after progressive demagnetization of the NRM of a minimum of 10 samples per site. The mean site direction, and the mean direction of groups of sites from the same structural unit were calculated. The fold test applied to a set of sites located on the Montsec thrust sheet gave positive results, indicating an age of the magnetization prior to deformation. However, evidence of postfolding magnetizations were found in other sites. The results of this study indicate significant counterclockwise rotations of the Cadí, Port del Comte, and the eastern termination of the Montsec thrust sheets, developed during the Mid Eocene to Oligocene times. These results are intended to contribute to the restitution of the initial geometry of the structures and to contribute to the paleogeographic reconstruction of the sedimentary systems of the eastern and central Pyrenees.

KEYWORDS **Paleomagnetism. Pyrenees. Tectonic rotation. Oroclinal bending.**

INTRODUCTION

Oroclines are intriguing features that are common in deformed regions on the earth surface, and are characterized by a prominent bending of the structural trend within an orogenic belt. They are frequent in the alpine belt, from the Himalayas to the Pyrenees, and their origin may be diverse, either related to the presence of a non-linear collisional front (primary arc) or a gradient of shortening along strike (secondary arc) (Eldredge *et al.,* 1985; Weil and Sussman, 2004). These are two end-member scenarios that may occur simultaneously, giving

rise to different gradients of progressive curvature during the formation of an orogen.

The study of oroclinal bending is crucial for the palinspastic restoration of collisional belts and the paleogeographic reconstruction of deformed regions. Since 2D sections cannot satisfactorily describe displacements caused by vertical axis rotations (Apotria, 1995; Sussman *et al.*, 2004, 2012; Willkerson *et al.*, 2002) a key tool to provide constraints on the 3D kinematics is paleomagnetism, as it provides reliable markers of vertical-axis rotations that affected the rocks upon deformation (Arriagada *et al.*, 2008; Bayona *et al.*, 2003; Pueyo *et al.*, 2003; Ramon *et al.*, 2012, 2016).

The South-Pyrenean fold-and-thrust belt offers the opportunity to study the origin of structures oblique to the main trend, and their relation to the emplacement of thrust nappes. A good case-study is the Aínsa Oblique Zone, where the rotational evolution could be constrained from the study of pre and syn-kinematic sediments deposited in the Aínsa basin. There, clockwise rotations of up to 70º occurring from early Lutetian to late Bartonian, are abundantly documented (Garcés *et al.*, 2016; Mochales *et al.*, 2012; Muñoz *et al.*, 2013; Pueyo *et al.*, 2022). Further south, the westward propagation of the deformation front along the Sierras Exteriores was found to co-occur with significant clockwise rotations (Pueyo *et al.*, 2002).

Paleomagnetic studies in the Pyrenees are, however, unevenly distributed or even lacking in regions such as the Segre Oblique Zone (SOZ). The work of Dinarès (1992) in the central and eastern part of the Bóixols and Montsec thrust sheets focused mainly on Jurassic and Cretaceous rocks and, to a lesser extent, on Eocene rocks. East of the Segre river, data available is sparse and distributed among different units, such as the Palaeogene of the Cadí thrust sheet in the Serra del Cadí (Pueyo *et al.*, 2016) and the Ripoll syncline (Burbank *et al.*, 1992a), the Garumnian facies of the Vallcebre syncline in the middle Pedraforca nappe (Oms *et al.*, 2007), the late Cretaceous of the Pedraforca Nappe (Keller *et al.*, 1994), in autochthonous Eocene-Oligocene rocks of the Busa syncline (Keller *et al.*, 1994) and the Oliana anticline (Burbank, Sussman *et al.*, 2004; Vergés *et al.*, 1992b). Therefore, paleomagnetic studies to constrain the vertical-axis rotations related to the evolution of the SOZ are insufficient.

This work aims at providing new paleomagnetic data from the SOZ in order to constrain vertical-axis rotations, and to determine the primary or secondary nature of the arc. This will contribute to a better understanding of the early Eocene paleogeography, and the sedimentary systems that routed across the eastern and central South-Pyrenean foreland.

GEOLOGICAL SETTING

The southern Pyrenees

The Pyrenean range is an East-West asymmetrical double wedge orogenic belt resulting from the north-directed convergence between the Iberian and Eurasian plates (Choukroune, 1989; Muñoz, 1992; Vergés *et al.*, 2002). Cross-sections based on seismic profiles show evidence that the Iberian plate has subducted under the Eurasian plate (Muñoz, 1992; Teixell *et al.*, 2018). Collision and partial subduction of the Iberian plate beneath the European plate lasted from the late Santonian (late Cretaceous) until the Oligocene-early Miocene (Vergés *et al.*, 1995). A southern thrust system developed on top of the subducting Iberian plate whereas a northern thrust system grew on top of the European plate (Vergés *et al.*, 1995). A minimum total shortening of 111km was estimated for the eastern Pyrenees (Grool *et al.*, 2018), 147km for the Central Pyrenees (Muñoz, 1992), and only 75-80km for the western Pyrenees (Teixell, 1998).

The southern wedge of the Pyrenees involves two major structural domains from north to south: the Axial Zone and the South-Pyrenean Zone (SPZ), bounded to the south by the pro-wedge foreland Ebro Basin, that sits on autochthonous basement of the Iberian plate (See Fig. 1). The Axial Zone consists of a south verging antiformal stack of mainly Hercynian basement rocks, subdivided into the Rialp, Orri, and Nogueres nappes, rooted in depth with the basal thrust of the South-Pyrenean Zone (Choukroune and ECORS Team, 1989; Muñoz, 1992). The central part of the South-Pyrenean Zone, traditionally known as the South Pyrenean Central Unit (SPCU, Séguret, 1972) is composed from north to south, of the Cotiella-Bóixols, Montsec, and Serres Marginals thrust sheets. Towards the Eastern Pyrenees, their respective equivalents are the Upper, Middle and Lower Pedraforca thrust sheets, forming the upper nappes. The lower nappes correspond to the Port del Compte and Cadí thrust sheets.

The South-Pyrenean thrust sheets involve a Mesozoic sediment cover which changes in facies and thickness depending on their original situation relative to the rifted Iberian margin (Muñoz *et al.*, 2018), and describes an overall wedge thinning towards the south. The general sequence includes Triassic evaporites, shales, and carbonates, Jurassic marine carbonates, and from the Lower Cretaceous to Palaeocene, a diversity of calcareous sandstones, siltstones and marine carbonates. Additionally, the lower nappes also involve Devonian to Permian basement rocks (Martínez *et al.*, 1988).

The thrust sheets in the South-Pyrenean Zone were emplaced in a piggy-back sequence from north to south. The Bóixols thrust sheet was emplaced during the Late

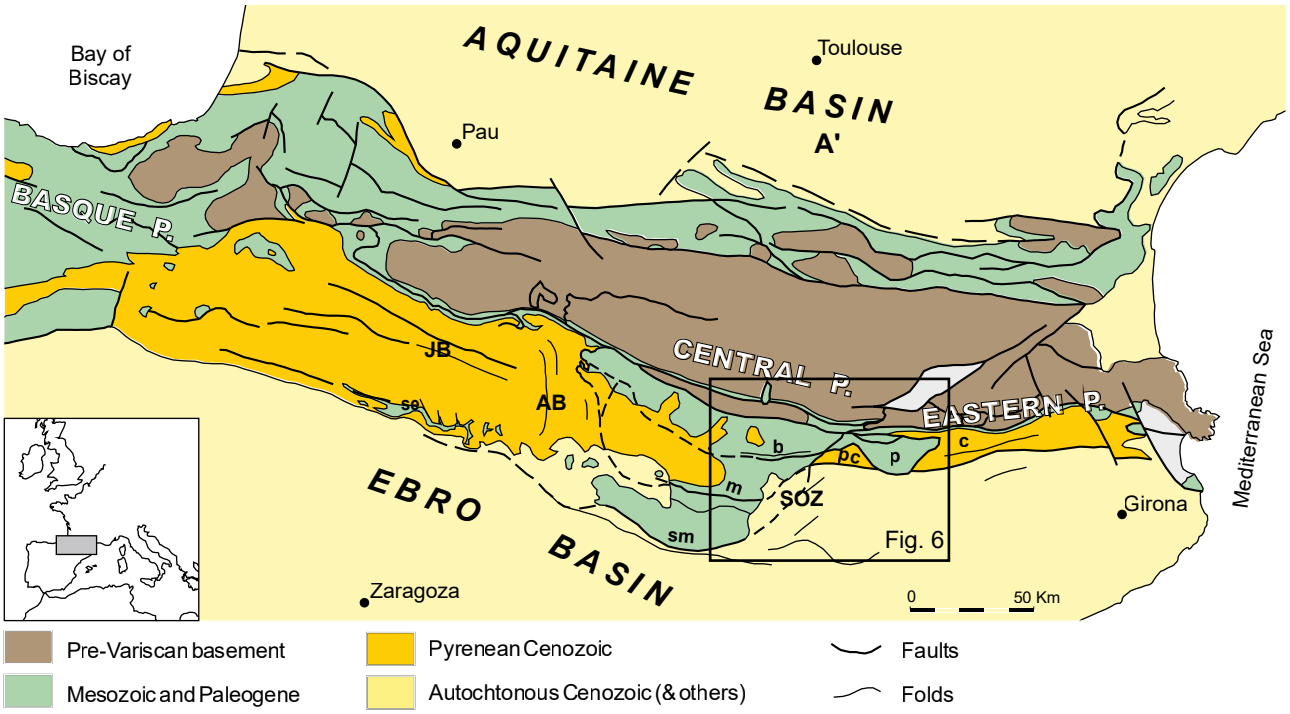

FIGURE 1. Geological map of the Pyrenees (Teixell, 1998). AB: Aínsa Basin, JB: Jaca Basin, SOZ: Segre Oblique Zone, se: Sierras Exteriores, b; Bóixols thrust sheet, m: Montsec thrust sheet, sm: Serres Marginals thrust sheet, pc: Port del Compte thrust sheet, p: Pedraforca thurst sheet, c: Cadí thrust sheet.

Cretaceous, followed by the Montsec thrust sheet, emplaced during the Palaeocene until the early Eocene, and finally the Serres Marginals, Port del Compte and Cadí thrust sheets emplaced from the Mid Eocene until Oligocene times (Muñoz *et al.*, 2013). This sequence of emplacements was coeval to the infill of the Tremp and Àger piggy-back basins with uppermost Cretaceous to Paleogene thick sedimentary sequences (Muñoz *et al.*, 2018).

The Segre Oblique Zone

The SPCU is a 90km long and 60km wide salient bounded to the east and west by zones of oblique structures. The Aínsa Oblique Zone, to the West, includes a set of blind thrusts and folds that formed under an accretionary margin with a relatively thick sediment accumulation during the Early-Mid Eocene. This contrasts with the SOZ to the east, characterised by uplift and erosion of the eastern termination of the SPCU thrust sheets (Vergés, 1989).

Originally known as the Segre fault (Garrido-Megías, 1973) or Catalunya fault (Séguret, 1972; Souquet *et al.*, 1977), these oblique structures were interpreted as a sinistral strike-slip movement along the eastern boundary of the SPCU. Others suggested deep faults of an older age, affecting the hercinian basement, and reactivated during the alpine deformation (Rosell and Robles, 1975). Garrido-Megías (1972) assigned an Eocene fault activity for the Segre fault. Later, the Isona and Comiols wells, drilled during oil exploration campaigns in the 1980s, revealed the presence of an autochthonous Eocene-Palaeocene sedimentary units beneath the Montsec thrust sheet. Correlation with seismic data made it possible to conclude that the basement units were not involved in the thrusts (Muñoz *et al.*, 2018), thus indicating that the SOZ corresponds to thin-skinned deformation of the sedimentary cover.

The term "lateral ramp" first appeared in the work of Simó and Puigdefàbregas (1985) and Cámara and Klimowitz (1985), while Clavell *et al.* (1988) suggested that these lateral ramps coincided with the paleogeographic boundary of a Mesozoic basin, as indicated by an isopach map from that period. Since then, the interpretation as oblique ramps prevailed, although terms such as "Segre alignment" or "Segre thrust" (Vergés and Muñoz, 1990) are often used to refer to these structures. These oblique ramps show a NE-SW cartographic trace, detaching from the Keuper and inverting a Mesozoic basin that pinches out towards the east. They thrust over the Port del Compte thrust sheet and the deformed foreland of the Ebro Basin (see Vergés, 2003 for more information).

Late Cretaceous-Early Eocene stratigraphic record

The Pyrenean orogeny began in the late Cretaceous, reactivating extensional faults and emplacing the Bóixols

and upper Pedraforca thurst sheets in the central and eastern Pyrenees. As a consequence, the Mesozoic marine strait that connected the Tethys and Atlantic progressively narrowed, leading to the emergence of the eastern region (Vergés *et al.*, 2002). The late Cretaceous and early Palaeocene sedimentary units record a regression in the pyrenean region, transitioning from a shallow marine environment with carbonate deposition to a clastic shallow marine environment (Areny Fm. and Perles Fm., see Fondevilla *et al.*, 2016; Oms *et al.*, 2007; Puértolas *et al.*, 2018 for detailed stratigraphic and magnetostratigraphic work) and finally to continental fluvial red mudstones and lacustrine carbonates of the Garumnian facies, including the Tremp Fm. (Puigdefàbregas *et al.*, 1992) (see Fig. 2). The Garumnian facies shows different characteristics according to the structural unit on which it was deposited. In the Vallcebre Basin (Lower Pedraforca Nappe), the Tremp Fm. is divided into four members (Rosell *et al.*, 2001): i) the grey Garumnian, composed of grey clays, lignites and interbedded sandstone and limestones deposited in a proximal marine environment; ii) the lower red Garumnian, made of fluvial palaeosol-bearing red mudstones and sandstones; iii) the Vallcebre limestone, composed of a massive unit of micritic lacustrine limestone rich in charophytes; iv) the upper red Garumnian is constituted of red palaeosoil-bearing mudstones, sandstones and lacustrine limestones with charophytes. The grey and lower red Garumnian are dated to the Maastrichtian in the Vallcebre Basin, and the Vallcebre limestone to the Danian (Oms and Canudo, 2004; Oms *et al.*, 2007). The age of upper red Garumnian is not very well constrained but since it is stratigraphically located between the Danian Vallcebre limestone and the early Eocene marine formations, its age would span from Danian to the earliest Eocene.

The Palaeocene-Eocene transition was characterized by a widespread transgression, leading to the expansion of shallow marine carbonate platforms, known as the Alveolina limestone, included in the Cadí Fm., which progressively evolved into the Penya Fm. During Eocene times, the formation of the south-Pyrenean foredeep led to a variety of depositional environments, resulting in the diversity of the stratigraphic record. The development of the SPCU salient interrupted the axial drainage system, preventing sediments from flowing longitudinally from the eastern Pyrenees to the Tremp-Graus basin, and enhancing sediment transfer across the Àger basin towards the Jaca Basin (Coll *et al.*, 2022; Garcés *et al.*, 2020; Gómez-Gras *et al.*, 2016; Juvany *et al.*, 2024b).

SAMPLING AND METHODS

The rocks sampled for this study embrace late Cretaceous shallow marine sediments, late-Cretaceous to Palaeocene (Garumnian) red beds, and early Eocene marine limestones. Garumnian red beds were preferentially targeted for two reasons. First, Palaeocene age sediments would record the total rotation accumulated during the compressional stage. Second, according to earlier studies (Juvany *et al.*, 2024a; Oms *et al.*, 2007) this lithology appears to hold a high intensity and stable remanence of primary origin. Continental red beds often yield a reliable paleomagnetic record as they have a high concentration of iron oxides that are stable under common oxidizing surface conditions.

The sampled outcrops were selected according to their structural simplicity, where the dip and polarity of the layers and the orientation of the fold axis could be determined. Fresh fine-grained sediments such as shales, marls, and micritic carbonates were targeted to avoid recent soil alteration. For each site, an average of 10 samples were collected from different layers. Cylindric samples of an average length of 10cm and 2.5cm diameter were collected using a water-cooled battery-powered drill and oriented in situ using magnetic compass mounted onto a core orienting fixture. Samples were cut into speciments of 2.1cm length in the laboratory using a disk saw.

The paleomagnetic study presented here is based on the determination of the Characteristic Remanent Magnetisation (ChRM) recorded in rocks. Provided that the ChRM is of primary origin (magnetization age corresponds to the age of rocks), the deviation of the remanence declination relative to the geographic north indicates that studied rocks underwent vertical-axis rotations. Magnetic measurements were conducted at the laboratory of paleomagnetism housed in the Geo3BCN Institute (CCiTUB-CSIC) in Barcelona. The measurement of the natural remanent magnetization (NRM) was conducted using a three-axis superconducting rock magnetometer SRM750 (2G enterprises). To isolate the different magnetic components, samples were subjected to progressive demagnetization treatment, either by increasing temperature steps (TH), or alternating magnetic fields (AF) (Beamud, 2012; Langereis *et al.*, 1989). Magnetic susceptibility was measured at each demagnetization step with a KLY-2 (Geofyzica Brno) to track mineralogical changes upon heating.

Since the behaviour of the rock's natural remanent magnetization during demagnetization depends on their magnetic mineralogy the samples were divided into groups according to rock type and a specific demagnetization routine were applied to them (Butler, 1998; Tarling, 1971). The samples from red-beds (continental), usually with abundant hematite, were all subjected to TH demagnetization up to temperatures close to 675ºC. Grey samples (marine or lacustrine), richer in magnetite, where subjected to both TH and AF demagnetization. TH demagnetization steps were

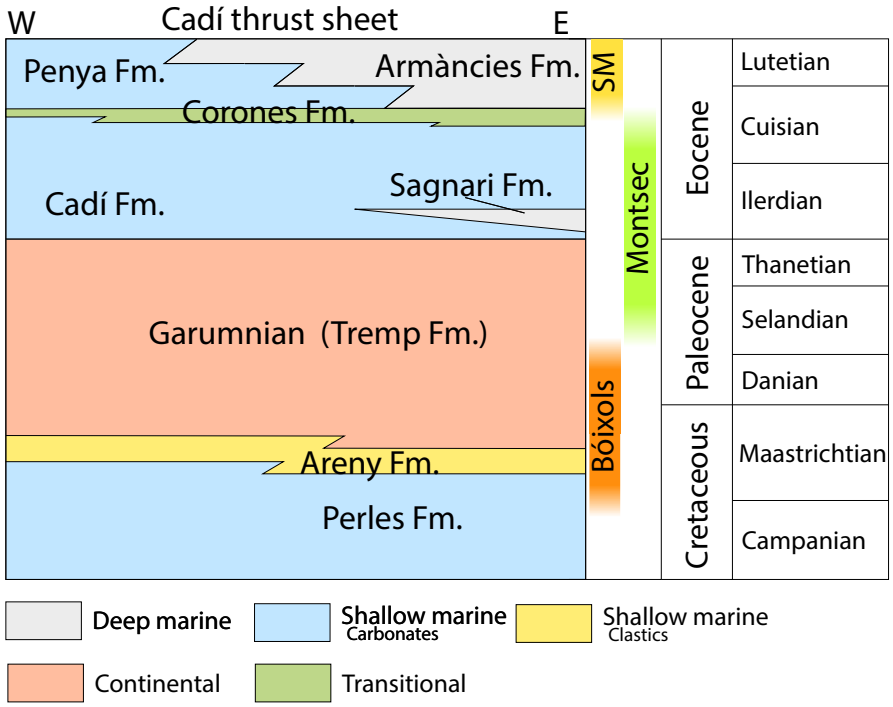

FIGURE 2. Simplified E-W stratigraphic chart of the main formations with the timing of the thrust sheet emplacements (Juvany *et al.*, 2024a).

at increments of 30-50ºC, and shorter when approaching the typical unblocking temperatures of minerals, to identify accurately the Characteristic Remanent Magnetization (ChRM) direction. AF demagnetization was carried out using a D-Tech 2000 demagnetizer, up to peak field of 120mT and an interval of progressive demagnetization ranging between 5 and 20mT.

The analysis of the ChRM was based on visual inspection of Zijderveld plots and paleomagnetic vectors were calculated using principal component analysis. ChRM components were identified after removal of viscous secondary magnetizations and were ranked according to their quality. Class I refers to ChRM components showing insignificant errors with linear nearly complete demagnetization trends towards the origin. Class II refers to ChRM components showing incomplete but linear demagnetization trend pointing toward the origin. Class III includes samples showing irregular demagnetization trends or clustered directions lacking a decay trend toward the origin.

Pmagpy software (Tauxe *et al.*, 2016) was used to carry out the calculations of paleomagnetic directions and to plot the results. The ChRM directions were projected on equal area stereonets and the mean direction was calculated for each site before and after tectonic correction. For the sake of comparison, the site mean directions were all flipped to normal polarity. To determine the relative age of the ChRM a regional fold test (Enkin, 2003) was performed on sites grouped by structural units. Paleomagnetic directions yielding a positive fold test were considered to pre-date the deformation and thus to behave as reliable markers of subsequent rotations.

Vertical-axis rotations were calculated relative to the nearest reference paleomagnetic direction in the Iberian plate. In the absence of Palaeocene-early Eocene data, an overall Cenozoic paleomagnetic direction from the Ebro basin of 002.3/42.8 (Pedrera *et al.*, 2023) was taken as the best reference for our study, implying the assumption of a stable Iberian plate during the Cenozoic. The associated error was calculated after Demarest (1983).

RESULTS

Natural Remanent Magnetization properties

Stepwise demagnetization of the NRM revealed different behaviour according to lithology. Campanian-Maastrichtian grey marly limestones of the Areny Formation (sites CN03 and GV01), exhibited erratic magnetizations, already noted by Dinarès (1992). The intensity of the NRM was weak (10^{-5}A/m) and the samples demagnetized at temperatures lower than 390ºC (Fig. 3A, B), making it difficult to reliably distinguish the ChRM components from viscous components. Demagnetization by alternating fields did not

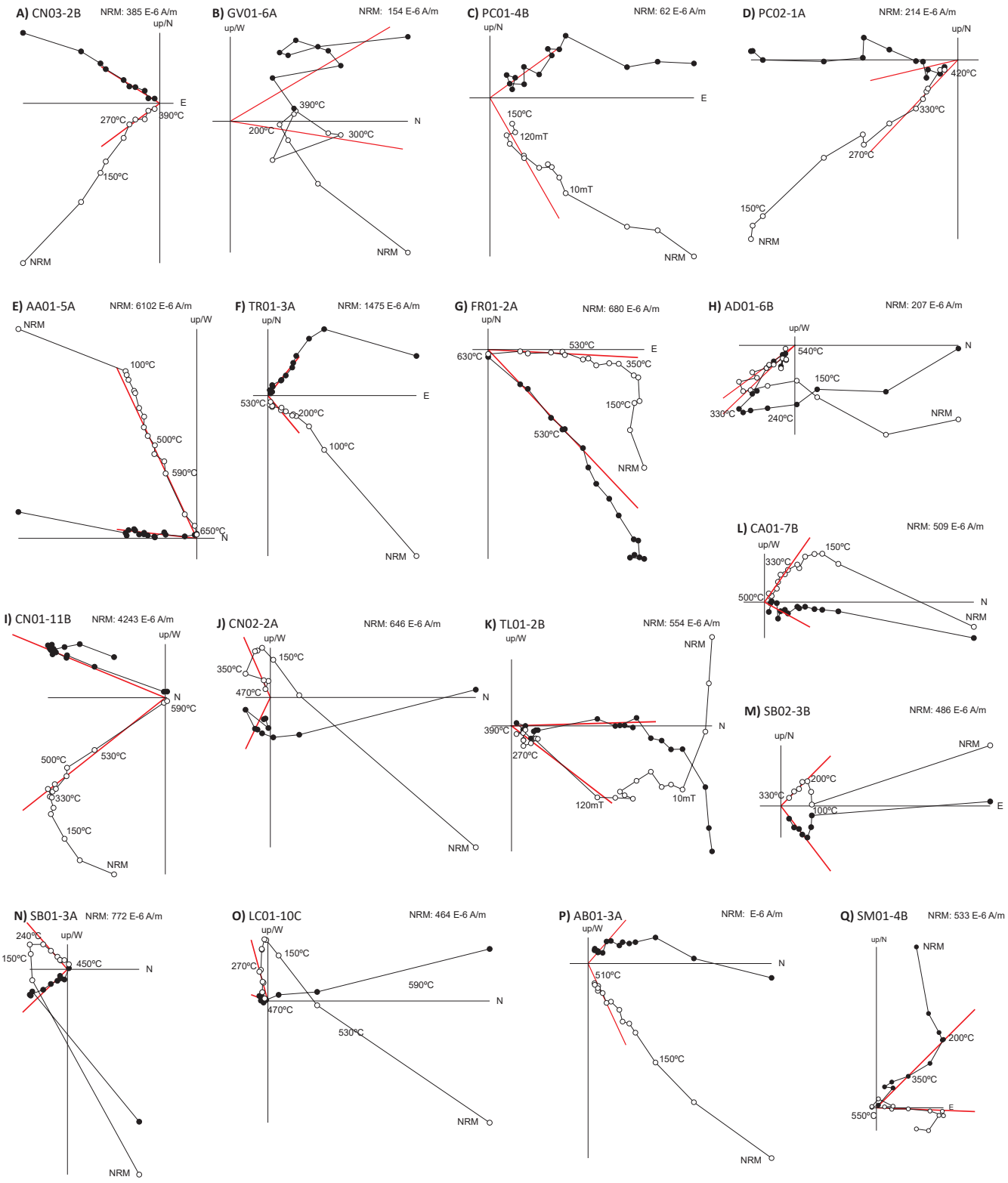

FIGURE 3. Stepwise demagnetization Zijderveld plots of representative samples. All plots are shown in geographic coordinates. AF: alternating field demagnetisation (mT), TH: Thermal demagnetisation (ºC). The black symbols correspond to the declination (projection on the horizontal plane) and the empty symbols to the inclination (projection on the vertical plane). The red lines represent the regression lines calculated for the characteristic component of the sample.

improve the results. A tendency of the ChRM to cluster about a northwesterly directed normal polarity direction was observed.

The Lutetian marine micritic limestones of the Penya Formation (sites PC01 and PC02) yielded low initial intensity of the NRM, ranging between 10^{-4} to 10^{-5}A/m and magnetic susceptibility of $2{\cdot}10^{-6}$ to 10^{-7}SI. Stepwise demagnetization showed the removal of the viscous components at 15mT (Fig. 3C) or 250ºC (Fig. 3D) that showed a large scatter. Above 250ºC, a ChRM component was identified with a gradually decreasing intensity between 350-500ºC (Fig. 3D). Both AF and TH treatment exhibited similar orientations and revealing dual polarity in PC01 and only normal polarity in PC02.

Sites AA01 and TR01 from the Pedraforca thrust sheet, along with AD01 and FR01 at the westernmost end of the Cadí Unit, were drilled in red mudstones with some intercalations of lacustrine limestones. At these sites, the initial Natural Remanent Magnetization (NRM) of the red mudstones exhibited high intensity(10^{-3}A/m) and magnetic susceptibility of the order of 10^{-5}SI. The north-directed viscous component was removed at temperatures of 250-300ºC and the ChRM component was revealed with straight demagnetization decay up to 630ºC (Fig. 3E, F, G, H), the majority of samples yielding a consistent reversed polarity after tectonic correction, and some of normal polarity. Limestone samples yielded poorer quality and component analysis for these was not completed.

Sites CN01, CN02 and TL01 from the Montsec thrust sheet, were drilled in Garumnian red mudstones and provided contrasting results. CN01 samples yielded high intensity and very stable ChRM components, demagnetized between 350ºC and 630ºC (Fig. 3I), and showing both normal and reversed polarities. However, these components yielded a large scatter of directions, both before and after bedding correction. CN02 yielded weaker ChRM components (Fig. 3J), consistent normal and reversed polarities after bedding correction although not properly antipodal, possibly due to partial overlap of recent viscous components. Lastly, TL01 (Fig. 3K) yielded very weak magnetization after heating to temperatures as low as 200ºC. The AF treatment of twin samples was unable to demagnetize the NRM completely, and further thermal treatment of these same samples revealed a normal polarity component with unblocking temperatures of 150ºC possibly carried by goethite.

Sites CA01, SB01, and SB02 (Fig. 3L, M, N) were drilled in Garumnian red mudstones and limestones of the Port del Comte thrust sheet. ChRM components were revealed after heating to 300ºC, and represented a low fraction of the NRM. They showed a large scatter of directions, but consistent with either reversed or normal polarities after bedding correction.

In the Serres Marginals thrust sheet sites AB01 and JN01 were drilled on massive limestones, and LC01 and SM01 on reddish mudstones. Among these only site LC01 (Fig. 3O) yielded coherent well defined ChRM components above 200ºC and directions consistent with a reversed polarity after beddind correction. Limestones of sites AB01 and JN01 (Fig. 3P) were weakly magnetized and their ChRM components were highly scattered. Red mudstones of SM01 (Fig. 3Q) had higher NRM intensity but ChRM components with a large scatter.

Site mean ChRM directions

The paleomagnetic directions were grouped according to their quality into three classes (see methods). Only five sites (TR01, AA01, FR01, AD01, and LC01) yielded enough ChRM directions of class I and II to calculate a robust mean site direction with a confidence cone that lower than 20º (Table 1; Fig. 4). In these sites, the addition of paleomagnetic directions of class III did not represent any significant improvement of the statistical parameters. Six sites (PC02, CN01, GV01, AB01, JN01, SM01) had few good quality directions and required the inclusion of class III. The resulting distribution yielded confidence cones ranging between 20º and 49º, too large errors to constrain local vertical-axis rotations, but were considered globally as in most cases the amount of net rotation was larger than the associated error (Table 1). Two sites (PC01, TL01) were excluded from calculation of vertical axis rotations and were not included in the summary table (Table 1). PC01 yielded too few directions, and incompatible with the neighbouring site PC02 of higher quality. TL01 had a remanence carried by goethite-type minerals, as the magnetization drops at low temperatures (150ºC) and is resistant to demagnetization by alternating fields. We interpret this remanence of likely secondary origin and therefore of uncertain age of magnetization. As the ChRM of TL01 is parallel to the present-day field, it could correspond to a recent remagnetization associated to surface alteration processes.

In general terms, sites with ChRM components of high quality (class I and II) yielded meaningful mean paleomagnetic directions with low associated errors. Site CN01 was an exception, yielding class I ChRM components but with a large scatter of directions. This site was drilled in a succession of vertical to overturned beds, forming part of the basal units of a growth-strata structure. Results from CN01 suggest that magnetization could have been locked soon after deposition but slightly delayed in each sample, and thus recording different stages of folding and causing the large scatter of directional data.

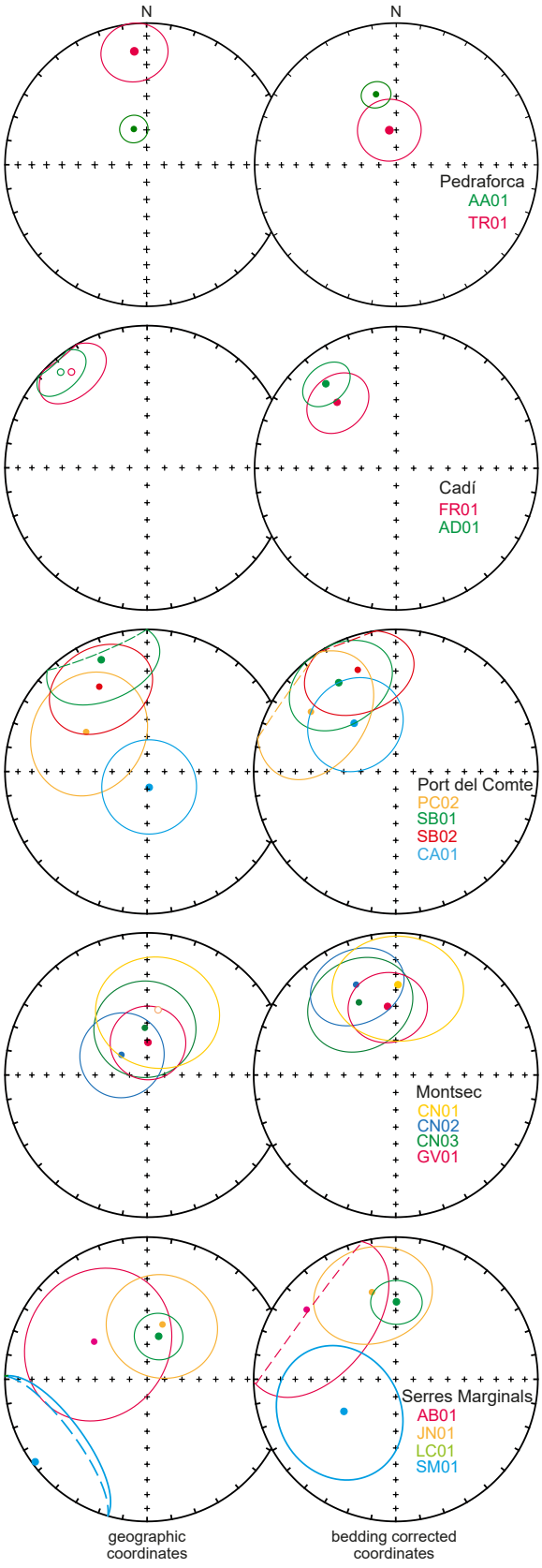

FIGURE 4. Stereographic projections of mean sites directions grouped by structural units.

DISCUSSION

Relative age of magnetization

Setting the age of magnetization is key to interpret paleomagnetic data (Van der Voo, 1990). The temporal relationship between the age of magnetization and rock deformation can be determined by testing the coherence of site mean directions relative to bedding. The overall coherence of paleomagnetic inclinations with the expected geomagnetic field inclination after bedding correction is an indication of early predeformational remanence acquisition (Fig. 4). Additionally, the presence of antipodal normal and reversed ChRM components in several sites points to an early remanence soon after deposition. Only sites CN02 and CA01 showed that directions of normal and reverse polarity were not entirely antipodal, with the normal polarity directions biassed towards the northwards directed present-day field. A partial overlap with a recent viscous component best explains this deflection of the ChRM components.

In this study, a fold test was carried out on sites of the Montsec thrust sheet GV01, CN01, CN02 and CN03 (Fig. 5). A significant increase in the grouping of data after bedding correction indicates a positive test, that is, that the remanence predates folding.

Post-folding magnetizations were only observed locally associated to a site affected by early synsedimentary folding (CN01). We interpret this as resulting from a delayed acquisition during early burial rather than a remagnetization event. Since beds underwent tilting soon after deposition, a delayed magnetization would be acquired syn-or post-folding. We therefore do not find here a relationship with a regional remagnetization process that might affect late Cretaceous and Cenozoic rocks in the Cadí thrust sheet suggested by others (Pueyo *et al.*, 2016) and related to the loading of the Pedraforca unit.

Vertical-axis rotations and structural implications

In general terms most sites show a clear north-westward orientation of their mean paleomagnetic directions, indicating a counter-clockwise rotation of all structural units involved in the SOZ (Fig. 6). Both Montsec and Serres Marginals thrust sheets present similar counterclockwise (CCW) rotation values, especially in those areas closer to the oblique ramps. The same coherency is found in the rotation values between the sites in the Port del Compte thrust sheet.

Further, no apparent gradient of rotation is observed between the lower and the upper nappes of the eastern Pyrenees. Note that sites of the Cadi and Port del Comte

TABLE 1. | Paleomagnetic site mean directions and corresponding statistics parameters in geographic and stratigraphic (bedding corrected) coordinates. For the sake of comparison, all directions are flipped to normal polarity. dipdir/dip: bedding dip direction and dip angle, * for overturned; n/N: ratio between calculated directions and total number of samples analysed; Pol.: ChRM polarity; Int.: ChRM intensity in 10^{-6}A/m; α_{95}: 95% confidence limit of the mean direction; k: Fisher precision parameter; Dg, Ig: ChRM declination and inclination in geographic coordinates; Ds, Is: ChRM declination and inclination in stratigraphic coordinates; r: vector sum of ChRM components. Net vertical axis rotation relative to a reference paleomagnetic declination of 002.3 (Pedrera *et al.*, 2023). Sites PC01 and TL01, considered of unreliable interpretation, were excluded from this summary table

		Site coordinates				Bedding	ChRM			Geographic coordinates		Stratigraphic coordinates					Net
Structural unit	Site	Latitude	Longitude	Rock unit	Lithology	dipdir/dip	n/N	Int.	Pol.	Dg	Ig	Ds	Is	α_{95}	k	r	rotation
Mid Pedraforca	TR01	42°13'5.25"N	1°43'11.66"E	Tremp Fm	Red shales	172/22	8/10	165	N/R	349.6	44.8	347.6	66.8	16.2	12.7	7.4	- 15±35
Low Pedraforca	AA01	42°12'3.79"N	1°27'3.16"E	Tremp Fm	Ochre shales	348/21	8/13	1470	R	340.3	68.1	343.9	47.2	8.0	48.6	7.9	**- 19±9**
Cadí	FR01	42°15'31.78"N	1°30'43.29"E	Tremp Fm	Red shales	158/55	7/10	216	R	321.7	-15.2	318.1	37.5	17.4	12.9	6.5	**- 45±17**
	AD01	42°16'57.91"N	1°32'3.65"E	Tremp Fm	Red shales	110/38	8/11	720	R	317.9	-10.2	320.2	23.4	12.8	19.6	7.6	**- 42±10**
Port del Comte	PC02	42°10'33.38"N	1°33'26.00"E	Penya Fm	Limestone	312/20	5/10	34	N	303.0	47.6	305.2	27.8	34.7	5.8	4.3	**- 57±30**
	SB01	42° 8'9.71"N	1°29'47.61"E	Tremp Fm	Limestones	221/28	9/10	51	R	337.7	16.1	327.3	26.6	27.2	4.5	7.2	**- 35±23**
	SB02	42° 8'56.32"N	1°31'4.50"E	Tremp Fm	Limestones	041/18	6/10	35	N/R	330.6	32.0	339.5	24.6	27.4	7.0	5.3	**- 23±23**
	CA01	42° 8'8.87"N	1°23'15.24"E	Tremp Fm	Ochre shales	326/45	11/11	233	N/R	172.3	80.9	319.3	53.0	27.2	3.8	8.4	**- 43±39**
Montsec	CN01	42°10'35.22"N	1°18'53.10"E	Tremp Fm	Red shales	335/81*	4/11	1799	R	009.6	-51.6	001.4	36.6	34.0	8.3	3.6	- 1±34
	CN02	42°10'20.88"N	1°17'53.35"E	Tremp Fm	Red shales	352/53	6/10	315	N/R	308.2	71.3	336.3	31.2	24.3	8.6	5.4	**- 26±22**
	CN03	42° 8'51.94"N	1°18'30.95"E	Perles Fm	Marly lst.	303/27	9/15	75	N/R	357.3	62.8	333.1	42.2	28.6	4.2	7.2	- 30±31
	GV01	42° 6'24.26"N	1°12'41.84"E	Areny Fm	Marls	345/22	4/11	67	N	353.0	44.4	351.1	22.5	49.4	4.4	3.3	- 12±43
Serres Marginals	AB01	41°54'43.71"N	0°57'9.58"	Tremp Fm	Limestones	313/31	5/10	42	N	305.4	52.3	308.0	21.5	43.7	4.0	4.0	**- 55±36**
	JN01	42° 5'33.64"N	1°16'23.68"E	Tremp Fm	Limestones	305/34	6/10	55	N/R	015.7	57.1	344.7	36.6	31.0	5.6	5.1	- 18±31
	LC01	41°57'24.83"N	1° 0'30.83"E	Tremp Fm	Ochre shales	340/22	10/11	165	R	015.1	64.4	000.5	44.7	13.6	13.7	9.3	- 2±15
	SM01	41°54'37.36"N	0°59'30.60"E	Tremp Fm	Ochre shales	044/48	8/9	315	N/R	233.7	02.6	239.1	49.6	37.8	3.1	5.8	**- 124±54**

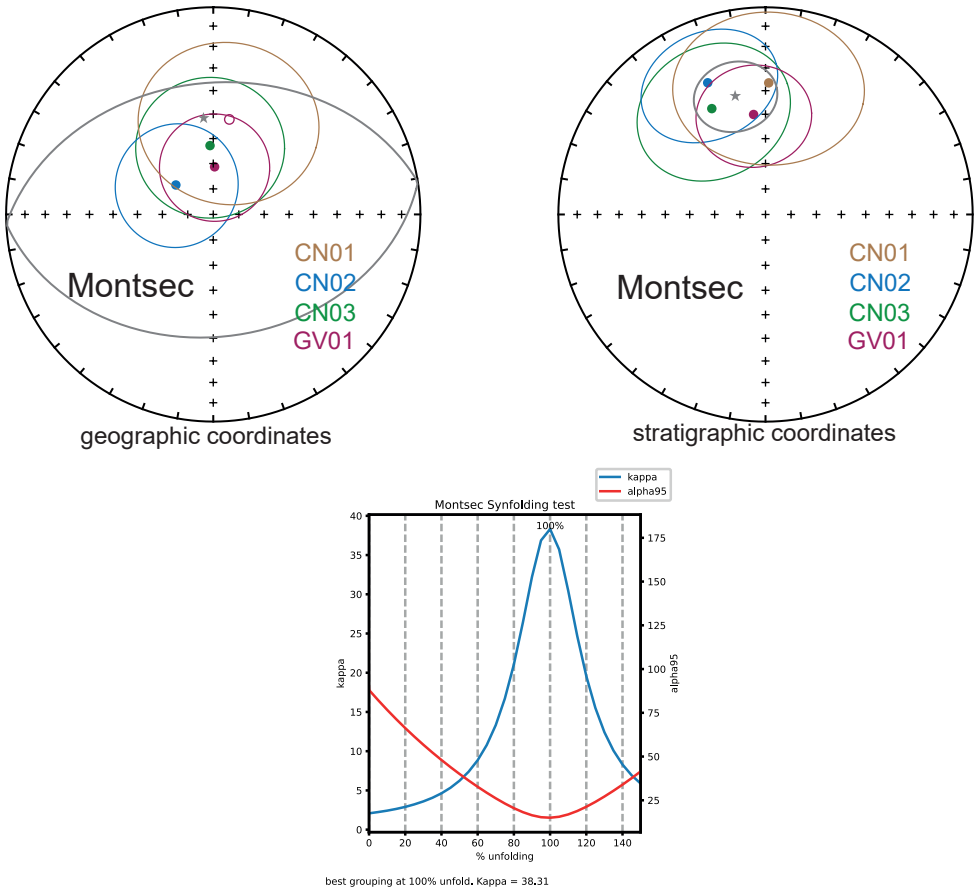

FIGURE 5. Fold test of paleomagnetic data from sites of the Montsec thrust sheet GV01, CN01, CN02 and CN03. The synfolding plot shows maxima of k and minima of α_{95} at 100% folding, indicating that the magnetization predates folding. The star indicates the mean vector calculated from the sites included in the Montsec thrust sheet.

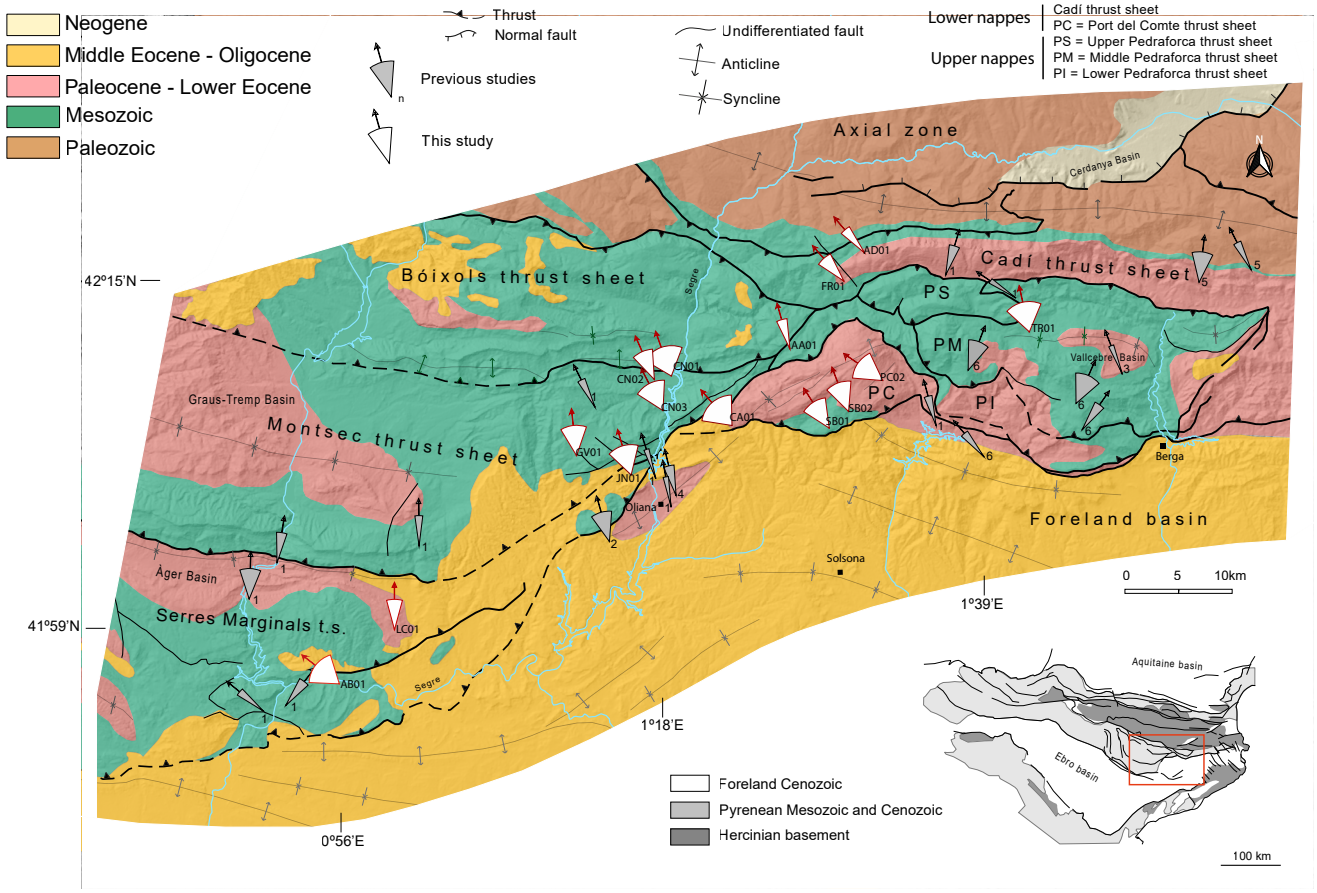

FIGURE 6. Structural map of the eastern SPZ with paleomagnetic data from this study and previous works. Base map modified from ICGC (2014) and Martínez *et al.* (2001). The arrows indicate the rotation value and associated error of each site (Table 1). Paleomagnetic data from others colored in grey and numbered as follow: 1: Dinarès (1992); 2: Burbank *et al.* (1992b); 3: Oms *et al.* (2007); 4: Sussman *et al.* (2004); 5: Pueyo *et al.* (2016) and 6: Keller *et al.* (1994).

thrust sheets, the lower and younger thrust sheets being emplaced, show as much as 45° CCW rotation, indicating that vertical-axis rotations equally affected all structural units, both in Palaeocene and Eocene rocks. These results not only indicate that vertical-axis rotation occurred in association with the emplacement of the lower nappes, but also prove that the main rotation event took place during Mid Eocene to Oligocene times.

The data from this study is consistent with previous results in the SPZ from Beamud *et al.* (2003); Dinarès (1992); Muñoz *et al.* (2013) and Sussman *et al.* (2004), reporting significant rotations associated to the occurrence of oblique structures and an attenuation of these rotations moving away from the oblique structures, towards the center of the SPZ, suggesting a gradient of tectonic a displacement. Here we provide evidence of rotations involving the western termination of the Cadí thrust sheet that was not previously considered. The sites located on the Port del Comte thrust sheet show significant counterclockwise rotations in the Eocene rocks. The sites closely located to the presumed oblique ramps do not show larger rotations as would be expected if the rotations were due to drag during the translation of the block over an oblique or lateral ramp (Dinarès *et al.*, 1992). Thus, despite the limited number of study sites, it appears to be a correlation between the amount of rotation and the strike of the tectonic structures on both ends of the SOZ (Fig. 7). The geographic extend of the area affected by rotations is not well constrained, and further data well distributed over the region would be required to constrain the domains affected and the amount of rotations.

From the results of this work it cannot be stated unequivocally that the curvature of the eastern edge of the SPCU is 100% secondary (Fig. 7). But the evidence of significant rotations allows the curvature of the SOZ to be classified as oroclinal, according to the criteria of Marshak (2004), challenging the former view of this region as a lateral ramp of the SCPU. The presence of large normal faults in the hangingwall of the oblique structures, mapped in the Montsec thrust sheet north of Oliana, indicates significant stretching of these structures in response to their increase in length (Muñoz *et al.*, 2013). In the footwall, Sussman *et*

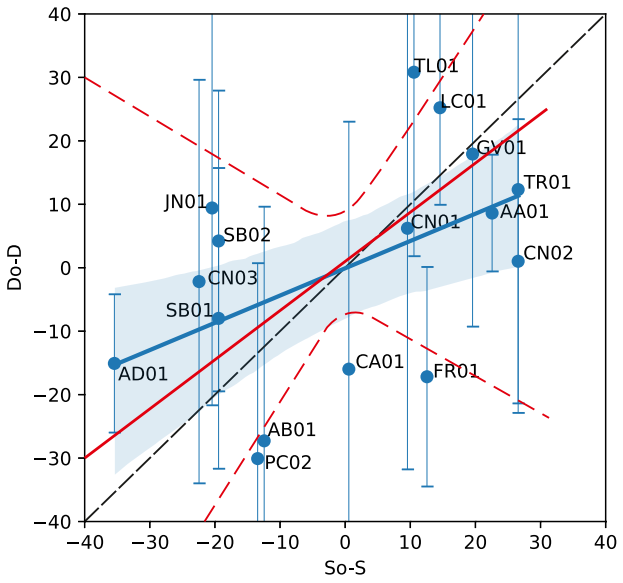

FIGURE 7. Projection of the site mean paleomagnetic declination as a function of the structural trend. D-Do: Difference between mean declination and site declination; S-So: Difference between the mean structural strike and the local strike at each site. The black stripped line corresponds to a 100% secondary arc. The blue line corresponds to the regression obtained from the sites with a 95% confidence interval. The red lines correspond to the bootstrapped confidence interval (Pastor-Galán *et al.*, 2017).

al. (2004) provided evidence of thrusting contemporaneous with rotation, implying the progressive curvature of the structures that developed in the autochthonous domain.

The general counterclockwise rotations observed along the structural units bounding the SOZ contribute to improve palinspastic restitutions of the South-Pyrenean foreland basin, and to better understand the relationships between adjacent subbasins, their depositional environments and the sedimentary routing systems can be better understood.

CONCLUSIONS

This work provides new insights on the behavior of magnetization and the rotational evolution of structural units in the Segre Oblique Zone:

i) Upper Cretaceous-Palaeocene red bed Garumnian facies are found to carry a high intensity stable prefolding magnetization. Interbedded lacustrine and palustrine carbonate facies yielded coherent results although directions showed a larger scatter.

ii) Paleomagnetic data indicates substantial counterclockwise rotations on both sides of the Segre Oblique Zone, affecting the Port del Comte thrust sheet, the eastern termination of the Montsec thrust sheet, the Serres Marginals thrust sheet, the westernmost end of the Cadí thrust sheet and the Pedraforca thrust sheets.

iii) The comparable rotation values among the thrust sheets suggest that the rotation was predominantly influenced by the lower nappes, which were emplaced during the Mid Eocene to Oligocene, thus providing a timeframe for the rotation.

iv) The data suggest that the curvature of the Segre Oblique Zone is secondary to some degree, but the large scatter of measurements does not allow to be precise on the amount of bending.

v) Results of this work will contribute to improve the palinspastic restoration of the SPZ and the paleogeographic evolution of the Pyrenean system after Palaeocene times.

ACKNOWLEDGMENTS

This is a contribution of the Marie Skłodowska-Curie Innovative Training Networks (H2020-MSCA-ITN-2019) Signal Propagation in Source to Sink for the Future of earth Resources and Energies (S2S-Future). Partially funded with Spanish project PID2019-106440GB-C21/AEI/10.13039/501100011033). We thank the Paleomagnetic Laboratory CCiTUB-Geo3Bcn CSIC for the support on paleomagnetic analysis. Thanks to Emilio L. Pueyo Morer, Ruth Soto and Antonio Teixell for the constructive reviews that helped improving the manuscript.

REFERENCES

Apotria, T.G., 1995. Thrust sheet rotation and out-of-plane strains associated with oblique ramps: An example from the Wyoming salient USA. Journal of Structural Geology, 17(5), 647-662.

Arriagada, C., Roperch, P., Mpodozis, C., Cobbold, P.R., 2008. Paleogene building of the Bolivian Orocline: Tectonic restoration of the central Andes in 2□D map view. Tectonics, 27(6), TC6014. DOI: https://doi.org/10.1029/2008TC002269

Bayona, G., Thomas, W.A., Van der Voo, R., 2003. Kinematics of thrust sheets within transverse zones: A structural and paleomagnetic investigation in the Appalachian thrust belt of Georgia and Alabama. Journal of Structural Geology, 25(8), 1193-1212.

Beamud, E., 2012. Paleomagnetism: Principles and applications. In Handbook of instrumental techniques for materials, chemical and biosciences research. Centres Científics i Tecnològics, Universitat de Barcelona, 9pp.

Beamud, E., Garcés, M., Cabrera, L., Muñoz, J.A., Almar, Y., 2003. A new middle to late Eocene continental chronostratigraphy

from NE Spain. Earth and Planetary Science Letters, 216(4), 501-514. DOI: https://doi.org/10.1016/S0012-821X(03)00539-9

Burbank, D.W., Puigdefàbregas, C., Muñoz, J.A., 1992a. The chronology of the Eocene tectonic and stratigraphic development of the eastern Pyrenean foreland basin, Northeast Spain. Geological Society of America Bulletin, 104(9), 1101-1120. DOI: https://doi.org/10.1130/0016-7606(1992)1042.3.CO;2

Burbank, D.W., Vergés, J., Muñoz, J.A., Bentham, P., 1992b. Coeval hindward- and forward-imbricating thrusting in the south-central Pyrenees, Spain; timing and rates of shortening and deposition. Geological Society of America Bulletin, 104(1), 3-17. DOI: https://doi.org/10.1130/0016-7606(1992)1042.3.CO;2

Butler, R.F., 1998. Paleomagnetism: Magnetic domains to geologic terranes. Blackwell Scientific Publications, University of Portland, 238pp.

Cámara, P., Klimowitz, J., 1985. Interpretación geodinámica de la vertiente centro-occidentalsurpirenaica. Estudios Geológicos, 41, 391-404.

Choukroune, P., ECORS Team, 1989. The ECORS Pyrenean deep seismic profile reflection data and the overall structure of an orogenic belt. Tectonics, 8(1), 23-39. DOI: https://doi.org/10.1029/TC008i001p00023

Clavell, C., Martínez, A., Vergés, J., 1988. Morfologia del basament del Pirineu oriental: Evolució i relació amb els mantells de corriment. Acta Geològica Hispànica, 23(2), 129-140.

Coll, X., Roigé, M., Gómez-Gras, D., Teixell, A., Boya, S., Mestres, N., 2022. Interplay of multiple sediment routing systems revealed by combined sandstone petrography and heavy mineral analysis in the South Pyrenean foreland basin. Minerals, 12(2), 262. DOI: 10.3390/min12020262

Demarest, H.H., 1983. Error analysis for the determination of tectonic rotation from paleomagnetic data. Journal of Geophysical Research: Solid Earth, 88(B5), 4321-4328. DOI: https://doi.org/10.1029/jb088ib05p04321

Dinarès, J., 1992. Paleomagnetisme a les unitats sudpirinenques superiors: Implicacions estructurals. Doctoral Thesis. Barcelona, Universitat de Barcelona, 447 pp.

Dinarès, J., McClelland, E., Santanach, P., 1992. Contrasting rotations within thrust sheets and kinematics of thrust tectonics as derived from palaeomagnetic data: An example from the Southern Pyrenees. In: McClay, K.R. (ed.). Thrust Tectonics. Springer, 265-275. DOI: https://doi.org/10.1007/978-94-011-3066-0_24

Eldredge, S., Bachtadse, V., Van der Voo, R., 1985. Paleomagnetism and the orocline hypothesis. Tectonophysics, 119(1-4), 153-179.

Enkin, R.J., 2003. The direction-correction tilt test: An all-purpose tilt/fold test for paleomagnetic studies. Earth and Planetary Science Letters, 212(1-2), 151-166. DOI: https://doi.org/10.1016/S0012-821X(03)00238-3

Fondevilla, V., Dinarès-Turell, J., Oms, O., 2016. The chronostratigraphic framework of the South-Pyrenean Maastrichtian succession reappraised: Implications for basin development and end-Cretaceous dinosaur faunal turnover. Sedimentary Geology, 337, 55-68.

Garcés, M., García-Senz, J., Muñoz, J.A., López-Mir, B., Beamud, E., 2016. Timing of magnetization and vertical-axis rotations of the Cotiella massif (Late Cretaceous, South Central Pyrenees). Geological Society Special Publication, 425(1), 213-232. DOI: https://doi.org/10.1144/SP425.11

Garcés, M., López-Blanco, M., Valero, L., Beamud, E., Anton, J., Oliva-Urcia, B., Vinyoles, A., Arbués, P., Cabello, P., Cabrera, L., 2020. Paleogeographic and sedimentary evolution of the South-Pyrenean foreland basin. Marine and Petroleum Geology, 113, 104105. DOI: https://doi.org/10.1016/j.marpetgeo.2019.104105

Garrido-Megías, A., 1972. Sobre la colocación del manto de Pedraforca y sus consecuencias: una nueva unidad tectónica independiente, "el manto del Montsec". Boletín Geológico y Minero, 83(3), 242-248.

Garrido-Megías, A., 1973. Estudio geológico y relación entre tectónica y sedimentación del Secundario y Terciario de la vertiente meridional pirenaica en su zona central (prov. Huesca y Lérida). Doctoral dissertation. Granada, Facultad de Ciencias, 395pp.

Gómez-Gras, D., Roigé, M., Fondevilla, V., Oms, O., Boya, S., Remacha, E., 2016. Provenance constraints on the Tremp Formation paleogeography (southern Pyrenees): Ebro Massif vs Pyrenees sources. Cretaceous Research, 57, 414-427.

Grool, A.R., Ford, M., Vergés, J., Huismans, R.S., Christophoul, F., Dielforder, A., 2018. Insights into the crustal-scale dynamics of a doubly vergent orogen from a quantitative analysis of its forelands: A case study of the eastern Pyrenees. Tectonics, 37, 450-476. DOI: https://doi.org/10.1002/2017TC004731

Institut Cartogràfic i Geològic de Catalunya (ICGC), 2014. Mapa estructural de Catalunya 1:250.000. Last accessed: October, 2024. Website: https://www.icgc.cat/Administracio-i-empresa/Descarregues/Cartografia-geologica-i-geotematica/Cartografia-geologica/Altres-mapes-geologics

Juvany, P., Garcés, M., Lopez-Blanco, M., Martín Closas, C., Beamud Amorós, E., Tosquella, J., Bekkevold, S.E., 2024a. Chronostratigraphy and tectono-sedimentary history of the eastern South Pyrenean foreland basin (Ripoll Syncline, North-East Spain). Depositional Record, 10(3), 338-363. DOI: https://doi.org/10.1002/dep2.287

Juvany, P., Garcés, M., López-Blanco, M., Valero, L., Amorós, E.B., Poyatos-Moré, M., Rius, A.M., 2024b. Unraveling the sediment routing systems evolution of the South Pyrenean foreland basin during the lower to middle Paleogene period. Marine and Petroleum Geology, 167, 106913. DOI: https://doi.org/10.1016/j.marpetgeo.2024.106913

Keller, P., Lowrie, W., Gehring, A., 1994. Palaeomagnetic evidence for post-thrusting tectonic rotation in the Southeast Pyrenees, Spain. Tectonophysics, 239(1), 29-42. DOI: https://doi.org/10.1016/0040-1951(94)90105-8

Langereis, C.G., Linssen, J.H., Mullender, T.A.T., Zijderveld, J.D.A., 1989. Demagnetisation. In: James, D.E. (ed.). The

Encyclopedia of Solid Earth Geophysics. Van Nostrand Reinhold Company, 201-211.

Martínez, A., Vergés, J., Muñoz, J.A., 1988. Secuencias de propagación del sistema de cabalgamientos de la terminación oriental del manto del Pedraforca y relación con los conglomerados sinorogénicos. Acta Geològica Hispànica, 23(2), 119-127.

Martínez, A., Berástegui, X., Losantos, M., Schöllhorn, E., 2001. Estructura de los mantos superior e inferior del Pedraforca (Pirineos orientales). Geogaceta, 30, 183-186.

Mochales, T., Casas, A.M., Pueyo, E.L., Barnolas, A., 2012. Rotational velocity for oblique structures (Boltaña anticline, Southern Pyrenees). Journal of Structural Geology, 35, 2-16. DOI: https://doi.org/10.1016/j.jsg.2011.11.009

Muñoz, J.A., 1992. Evolution of a continental collision belt: ECORS-Pyrenees crustal balanced cross-section. In: McClay, K.R. (ed.). Thrust tectonics. Springer Netherlands, 235-246. DOI: https://doi.org/10.1007/978-94-011-3066-0_21

Muñoz, J.A., Beamud, E., Fernández, O., Arbués, P., Dinarès, J., Poblet, J., 2013. The Ainsa Fold and thrust oblique zone of the central Pyrenees: Kinematics of a curved contractional system from paleomagnetic and structural data. Tectonics, 32(5), 1142-1175. DOI: https://doi.org/10.1002/tect.20070

Muñoz, J.A., Mencos, J., Roca, E., Carrera, N., Gratacós, O., Ferrer, O., Fernández, Ò., 2018. The structure of the South-Central-Pyrenean fold and thrust belt as constrained by subsurface data. Geologica Acta, 16(4), 439-460. DOI: https://doi.org/10.1344/GeologicaActa2018.16.4.7

Oms, O., Canudo, J.I., 2004. Datación magnetoestratigráfica de los dinosaurios del Cretácico terminal (Maastrichtiense superior) de Arén (Huesca, Unidad Surpirenaica Central). Geo-Temas, 6(5), 51-54.

Oms, O., Dinarès, J., Vicens, E., Estrada, R., Vila, B., Galobart, À., Bravo, A.M., 2007. Integrated stratigraphy from the Vallcebre Basin (southeastern Pyrenees, Spain): New insights on the continental Cretaceous–Tertiary transition in southwest Europe. Palaeogeography, Palaeoclimatology, Palaeoecology, 255(1), 35-47. DOI: https://doi.org/10.1016/j.palaeo.2007.02.039

Pastor-Galán, D., Mulchrone, K.F., Koymans, M.R., van Hinsbergen, D.J., Langereis, C.G., 2017. Bootstrapped total least squares orocline test: A robust method to quantify vertical-axis rotation patterns in orogens, with examples from the Cantabrian and Aegean oroclines. Lithosphere, 9(3), 499-511.

Pedrera, A., García-Senz, J., Pueyo, E.L., López-Mir, B., Silva-Casal, R., Díaz-Alvarado, J., 2023. Inhomogeneous rift inversion and the evolution of the Pyrenees. Earth-Science Reviews, 245, 104555. DOI: https://doi.org/10.1016/j.earscirev.2023.104555

Puértolas-Pascual, E., Arenillas, I., Arz, J.A., Calvín, P., Ezquerro, L., García-Vicente, C., Canudo, J.I., 2018. Chronostratigraphy and new vertebrate sites from the upper Maastrichtian of Huesca (Spain), and their relation with the K/Pg boundary. Cretaceous Research, 89, 36-59.

Pueyo, E.L., Millán, H., Pocoví, A., 2002. Rotation velocity of a thrust: A paleomagnetic study in the External Sierras (Southern Pyrenees). Sedimentary Geology, 146(1-2), 191-208. DOI: https://doi.org/10.1016/S0037-0738(01)00172-5

Pueyo, E.L., Pocoví, A., Parés, J.M., Millán, H., Larrasoaña, J.C., 2003. Thrust ramp geometry and spurious rotations of paleomagnetic vectors. Studia Geophysica et Geodaetica, 47, 331-357.

Pueyo, E.L., Beamud, E., Muñoz, J.A., Rodríguez-Pintó, A., San Miguel, G., 2016. Remagnetización alpina en la Serra del Cadí (Pirineo Oriental). Huelva, IX Congreso Geológico de España, 869-872.

Pueyo, E.L., Rodríguez-Pintó, A., Serra-Kiel, J., Barnolas, A., 2022. The chronology and rotational kinematics in the South-Eastern Jaca Basin (Southern Pyrenees): Las Bellostas section. Geologia Acta, 20(12), 1-29. DOI: https://doi.org/10.1344/GeologicaActa2022.20.12

Puigdefàbregas, C., Muñoz, J.A., Vergés, J., 1992. Thrusting and foreland basin evolution in the southern Pyrenees. In: McClay, K.R. (ed.). Thrust tectonics. Netherlands, Springer, 247-254.

Ramón, M.J., Pueyo, E.L., Briz, J.L., Pocoví, A., Ciria, J.C., 2012. Flexural unfolding of horizons using paleomagnetic vectors. Journal of Structural Geology, 35, 28-39.

Ramón, M.J., Pueyo, E.L., Caumon, G., Briz, J.L., 2016. Parametric unfolding of flexural folds using palaeomagnetic vectors. London, The Geological Society, 425(1, Special Publications), 247-258.

Rosell, J., Robles, S., 1975. Le Paléogène marin de la Catalogne. Bulletin de la Société Géologique de France, 7(XVII), 2, 195-198.

Rosell, J., Linares, R., Llompart, C., 2001. El "garumniense" prepirenaico. Revista de la Sociedad Geológica de España, 14(1-2), 47-56.

Séguret, M., 1972. Étude tectonique des nappes et séries décollées de la partie centrale du versant sud des Pyrénées. Publications de l'USTELA, Montpellier, Série Géologie Structurale, 2, 155pp.

Simó, A., Puigdefàbregas, C., 1985. Transition from shelf to basin on an active slope, upper Cretaceous, Tremp area, southern Pyrenees. Lerida (Spain), Excursion guide-book for the 6th European Regional Meeting, 63-108.

Souquet, P., Peybernès, B., Bilotte, M., Debroas, E.J., Rey, J., Canerot, J., 1977. Nouvelle esquisse structurale des Pyrénées. Toulouse, Publications de l'Université Paul Sabatier, Série Géologie, 8, 1-16.

Sussman, A.J., Butler, R.F., Dinarès, J., Vergés, J., 2004. Vertical-axis rotation of a foreland fold and implications for orogenic curvature: An example from the Southern Pyrenees, Spain. Earth and Planetary Science Letters, 218(3), 435-449. DOI: https://doi.org/10.1016/S0012-821X(03)00644-7

Sussman, A.J., Pueyo, E.L., Chase, C.G., Mitra, G., Weil, A.B., 2012. The impact of vertical-axis rotations on shortening estimates. Lithosphere, 4(5), 383-394.

Tarling, D.H., 1971. Principles and applications of palaeomagnetism. London, Chapman and Hall, 160pp.

Teixell, A., 1998. Crustal structure and orogenic material budget in the west central Pyrenees. Tectonics, 17, 395-406. DOI: https://doi.org/10.1029/98TC00561

Teixell, A., Labaume, P., Ayarza, P., Espurt, N., de Saint Blanquat, M., Lagabrielle, Y., 2018. Crustal structure and evolution of the Pyrenean-Cantabrian belt: A review and new interpretations from recent concepts and data. Tectonophysics, 724-725, 146-170. DOI: https://doi.org/10.1016/j.tecto.2018.01.009

Vergés, J., 1989. Estudi de la sedimentació i de l›estructura en el davant del mantell del Pedraforca: Evolució de la conca de l›Eocè sud-pirinenc. Doctoral dissertation. Barcelona, Universitat de Barcelona, 180pp.

Vergés, J., 2003. Evolución de los sistemas de rampas oblicuas de los Pirineos meridionales: fallas del Segre y Pamplona. Boletín Geológico y Minero, 114(1), 87-101.

Vergés, J., Muñoz, J.A., 1990. Thrust sequence in the southern central Pyrenees. Bulletin de la Société Géologique de France, 6(2), 265-271. DOI: https://doi.org/10.2113/gssgfbull.VI.2.265

Vergés, J., Millán, H., Roca, E., Berástegui, X., García-Senz, J., García-Vila, M., Santanach, P., 1995. Eastern Pyrenees and related foreland basins: Pre-, syn- and post-collisional crustal-scale cross-sections. Marine and Petroleum Geology, 12(8), 903-915.

Vergés, J., Fernández, M., Martínez, A., 2002. The Pyrenean orogen: Pre-, syn-, and post-collisional evolution. Journal of the Virtual Explorer, 8, 55-74. DOI: https://doi.org/10.3809/jvirtex.2002.00058

Weil, A.B., Sussman, A.J., 2004. Classifying curved orogens based on timing relationships between structural development and vertical-axis rotations. In: Sussman, A.J., Weil, A.B. (eds.). Orogenic curvature: Integrating paleomagnetic and structural analyses. Geological Society of America, 383, 1-15.

Wilkerson, M.S., Apotria, T., Farid, T., 2002. Interpreting the geologic map expression of contractional fault-related fold terminations as a function of fault geometry and displacement distance. Journal of Structural Geology, 24(4), 593-607. DOI: https://doi.org/10.1016/S0191-8141(01)00108-5

Manuscript received April 2024;
revision accepted November 2024;
published Online December 2024.